

## Measurement of the $W^+W^-$ pair production cross section in $\bar{p}p$ collisions at $\sqrt{s} = 1.96$ TeV

---

**Lee Pondrom\*** for the CDF Collaboration with special thanks to Will Parker and Matt Herndon

*University of Wisconsin, Madison*

*E-mail: pondrom@fnal.gov*

$W^+W^-$  can be produced directly by triple gauge coupling:  $\bar{q}q \rightarrow \gamma, Z \rightarrow WW$ , or as decay products of standard model Higgs bosons or  $\bar{t}t$  pairs. The Tevatron search for the decay  $H \rightarrow W^+W^-$  led to refinement of the techniques for isolating the  $W$  pair signal. At  $\sqrt{s} = 1.96$  TeV the cross sections for direct  $W$  pairs and  $\bar{t}t$  are comparable. This means that the direct production of  $W$  pairs with jets has a large background from top quarks. This measurement used the full Tevatron run II integrated luminosity of  $9.7\text{fb}^{-1}$ , and identified  $W$ 's by leptonic decay  $W^+ \rightarrow l^+ + \nu_l$ , giving the final state  $l^+l^- + \cancel{E}_T$ , where the charged lepton is either an electron or a muon. The measured total cross section is  $\sigma(p\bar{p} \rightarrow W^+W^- + X) = 14.0 \pm 0.6(\text{stat})_{-1.0}^{+1.2}(\text{syst}) \pm 0.8(\text{lumi})$  pb, consistent with the Standard Model prediction.

*XXII International Baldin Seminar on High Energy Physics Problems  
September 15-20, 2014  
JINR, Dubna, Russia*

---

\*Speaker.

**Table 1:** Previous Measurements of the WW Pair Cross Section

$\sqrt{s}$	Expt	Lum	$\sigma(\text{meas})$	$\sigma(\text{theory})$	Jets
1.96 TeV	D0	$1.1\text{fb}^{-1}$	$11.5 \pm 2.2\text{pb}$	$12.7 \pm 0.7\text{pb}$	incl
1.96 TeV	CDF	$3.6\text{fb}^{-1}$	$12.1 \pm 1.8\text{pb}$	$11.7 \pm 0.7\text{pb}$	veto $E_T > 15\text{ GeV}$
7 TeV	ATLAS	$4.6\text{fb}^{-1}$	$51.9 \pm 4.8\text{pb}$	$44.4 \pm 2.8\text{pb}$	veto $p_T > 25\text{ GeV}$
7 TeV	CMS	$4.9\text{fb}^{-1}$	$52.4 \pm 5.1\text{pb}$	$47.0 \pm 2.0\text{pb}$	veto $E_T > 30\text{ GeV}$
8 TeV	ATLAS	$20.3\text{fb}^{-1}$	$71.4 \pm 5.6\text{pb}$	$58.7 \pm 3.0\text{pb}$	veto $p_T > 25\text{ GeV}$
8 TeV	CMS	$3.5\text{fb}^{-1}$	$69.9 \pm 7.0\text{pb}$	$57.3 \pm 2.3\text{pb}$	veto $E_T > 30\text{ GeV}$

## 1. Introduction

W pair production is a test of the electroweak sector of the Standard Model, and an important background to searches for  $H \rightarrow W^+W^-$ . W pair production with one or more jets tests QCD predictions of jet production in a high mass electroweak process.[1] Multijet cross sections are complicated by the large top quark background, and for this reason most previous measurements have imposed a veto on jet activity. W pair cross sections have been reported by the CDF Collaboration [2], and the D0 Collaboration [3] for  $\bar{p}p$  collisions at 1.96 TeV, by the Atlas [4] [5], and CMS [6] [7] Collaborations for pp collisions at 7 TeV, and 8 TeV respectively. These results are summarized in Table I.

The first entry, by the D0 Collaboration, was the only inclusive measurement. The other experiments suppressed the top quark contribution by vetoing on accompanying jet energy. At 1.96 TeV the top quark cross section is about 1/2 of the W pair cross section, but at 7 TeV the top quark cross section is 3/2 of the W pairs, so the top background in W pairs plus jets is substantially larger at the LHC. In this report W pair cross sections were obtained for no jets, one jet, and two or more jets. A jet was defined by a cluster of transverse energy in the CDF II calorimeters:  $E_T = \sum_i E_i \sin\theta_i$ , summed over all calorimeter towers  $i$  in a cone of 0.4 in  $(\eta, \phi)$  space. The jet energy threshold is chosen  $E_T > 15\text{ GeV}$ , after applying the standard jet energy corrections package [8]. Events with no jets are free of top quark background. The one jet sample is divided into three bins in transverse energy:  $15\text{ GeV} < E_T < 25\text{ GeV}$ ;  $25\text{ GeV} < E_T < 45\text{ GeV}$ ; and  $E_T > 45\text{ GeV}$ . Three neural networks were trained for events with zero, one, and two or more jets to separate W pair events from backgrounds. The inputs to the neural nets were kinematic variables chosen for discrimination between signal and background, and generated by the simulation. The cross section for W pairs was extracted by allowing it to float in a likelihood fit of signal plus background to the neural net output shape.

## 2. Event Selection

The definitions of the physics objects were the same as those used by CDF in a previous search for  $H \rightarrow W^+W^-$  [9]. Trigger paths were central ( $|\eta| < 1$ ) high  $p_T > 18\text{ GeV}/c$  muons or central/forward ( $|\eta| < 2$ ) high  $E_T > 18\text{ GeV}$  electrons. All combinations  $(\mu, \mu)$ ,  $(\mu, e)$ ,  $(e, \mu)$ , and  $(e, e)$ , where the first lepton was the trigger, were accepted. Care was taken to avoid duplicate events. Any event with an identified cosmic ray track was eliminated. After full event reconstruction the trigger lepton was required to have  $p_T > 20\text{ GeV}/c$ , and the second lepton of opposite charge

$p_T > 10$  GeV/c. The missing transverse energy is an important variable in selecting decays  $W \rightarrow l\nu$ .  $\cancel{E}_T$  was calculated from the vector sum of all of the calorimeter tower transverse energies in the event:  $\cancel{E}_{Tx} = -\sum_i E_{Ti} \cos(\phi_i)$ , and similarly for the y component. This prescription should treat electron events, which deposit all of their energy in the calorimeters, correctly. Muon events, which deposit only minimal energy in the calorimeters, had to be treated separately. The muon transverse momentum vector was subtracted, and the calorimeter energy deposits (dE/dx by the muon track) were canceled in the tower sum to form the missing  $E_T$ . The missing  $E_T$  represented energy carried off by neutrinos, but also possible mismeasurement of hadronic and electromagnetic energy in the event, due to fluctuations in energy deposited, or gaps in the coverage of the calorimeters. For a W pair event, it was possible for the two neutrinos to cancel each other out, leading to a loss of data from a missing  $E_T$  requirement. In order to decrease the sensitivity to energy mismeasurement, if the missing  $E_T$  was within  $\Delta\phi = \pi/2$  of either a charged lepton or a jet, it was decreased by the factor  $\sin\Delta\phi$ . The cut requirement was  $\cancel{E}_T > 25$  GeV, relaxed to 15 GeV in (e, $\mu$ ) or ( $\mu$ ,e) events. Events with two or more jets were subjected to a secondary vertex tagger called HOBIT [10], which tags b quark decays with about a 30% efficiency. Since a  $t\bar{t}$  event has two b quarks, the probability of missing both of them, and leaving the top quark event in the sample, is about 50%.

### 3. Backgrounds

Top quark events remaining after the b tagger were an irreducible background in the W pair plus jets data. Other backgrounds came from various ways to fake the  $l^+l^- + \text{missing } E_T$  signature. One source is called 'Drell-Yan', and refers to the background from  $\bar{p}p \rightarrow e^+e^-, \mu^+\mu^-, \text{ or } \tau^+\tau^-$  decays. For Drell-Yan to make it into the data sample, there had to be missing  $E_T$  from mismeasurement. For (e,e) and ( $\mu$ , $\mu$ ) events a cut was made on the dilepton mass  $80 \text{ GeV} < M_{ll} < 99 \text{ GeV}$  to remove background from Z decays. This cut was not necessary in the (e, $\mu$ ) sample. There were about 1000 times as many single W's produced as W pairs. Single W's have only one high  $p_T$  neutrino, hence plenty of missing  $E_T$ , but they lack the extra opposite sign lepton. Therefore to make it into the data sample, the single W event had to fake a lepton. This could be done from W + jets data, where the 'jet' satisfied either the electron or muon identification, or from W+ $\gamma$  events, where the  $\gamma$  converted into an ( $e^+e^-$ ) pair, and only one electron was observed. The 'jet' that faked a lepton was a peculiar jet, because the leptons were required to be isolated. One possibility was a fragmentation fluctuation into a single  $\pi^0$  for a fake electron, or a single  $\pi$  or K decay in flight for a muon - a real muon, but a fake signature for our purposes. The same sign dileptons were one handle on the single W background.  $W \rightarrow e\nu + \gamma$  or  $\mu\nu + \gamma$  cross section is about 19 pb.[11] The WZ and ZZ backgrounds were modeled using PYTHIA [12]. WZ and ZZ cross sections are smaller than WW.

### 4. Analysis

The WW signal and the modeling of the various backgrounds as a function of the jet activity are shown in Figure 1. Figure 2 shows the same plot for same sign dileptons. Note that the y axis scale has changed by a factor of 2.5. The W $\gamma$  contributions to the zero jet bin are equal - about 200 events.  $D - Y \rightarrow \tau^+\tau^-$  is the dominant source for D-Y in the same sign plot. The opposite sign plot

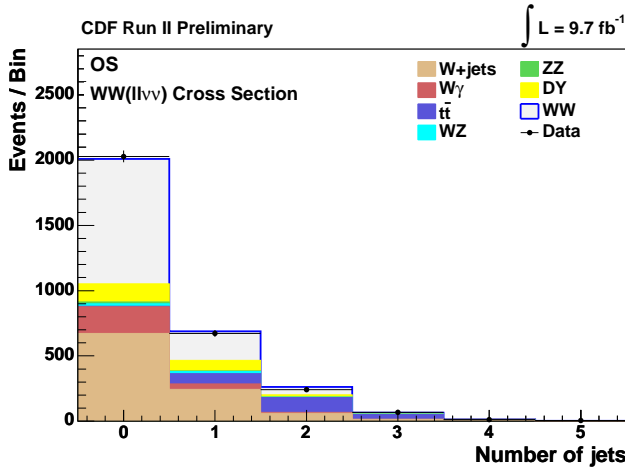


**Figure 1:** Plot of the components of signal plus backgrounds for opposite sign dileptons as a function of the number of jets.

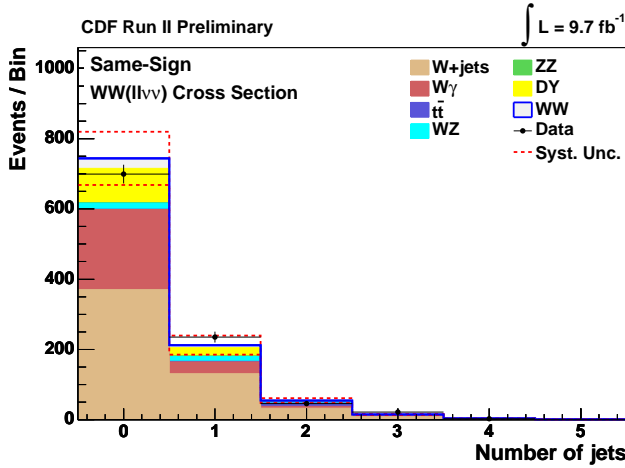


**Figure 2:** Plot of the components of signal plus backgrounds for same sign dileptons as a function of the number of jets.

shows that the W pair signal is about half of the total - the signal to noise is one to one, at least in the zero and one jet bins. The top quarks make no contribution to the zero jet bin, but dominate in two or more jets. These plots show that the measurement of the W pair cross section in the zero jet bin is straightforward, but becomes more difficult for two or more jets.

The NeuroBayes [13] network was trained on ten kinematic variables representing monte carlo modeling of signal plus backgrounds. Two of these variables, the dilepton invariant mass and the missing  $E_T$  are shown for zero jets in Figures 3 and 4; for one jet in Figures 5 and 6, and for same sign in Figures 7 and 8.

Figures 3,5, and 7 clearly show the cut from 80 to 100 GeV to eliminate  $Z \rightarrow l^+l^-$  decays. The  $(e,\mu)$  events fill this gap. The average transverse mass and missing  $E_T$  are higher for opposite sign events. Other kinematic variables also display signal/background differences, allowing the neural net to distinguish between them. The  $p_T$  of the second lepton is softer in the background. The total

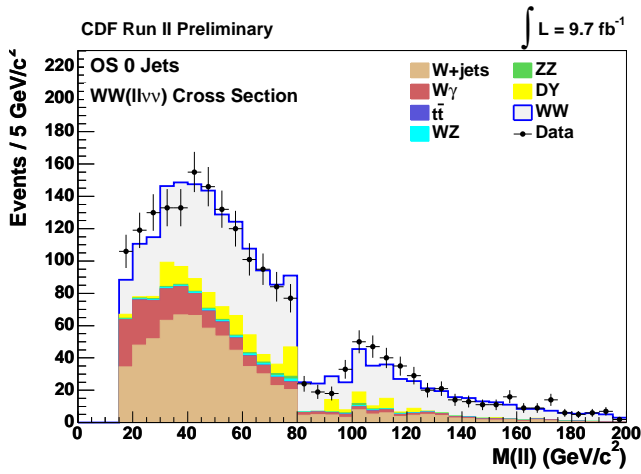


Figure 3: Plot of the invariant mass of the opposite sign lepton pair for zero jet events.

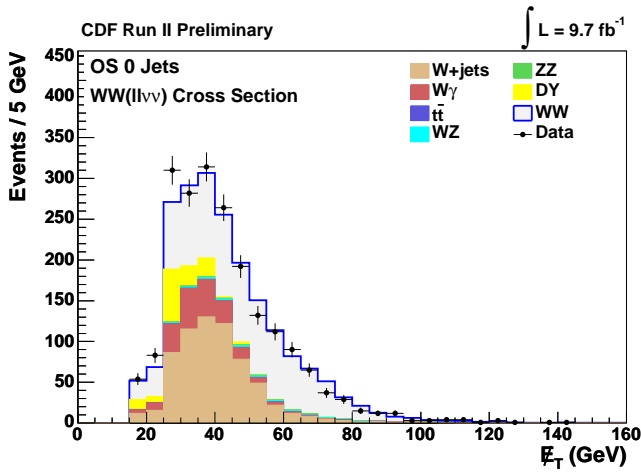


Figure 4: Plot of the missing  $E_T$  for opposite sign dileptons with zero jets.

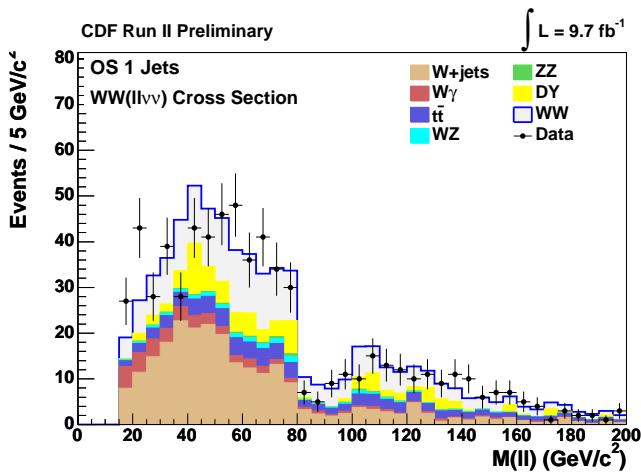


Figure 5: Plot of the invariant mass of the opposite sign lepton pair with one jet.

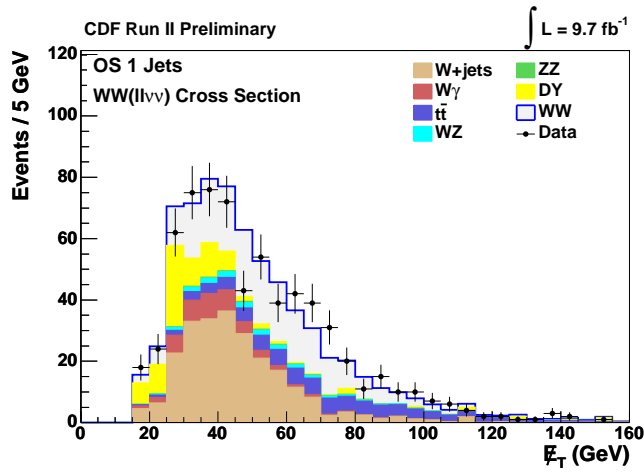


Figure 6: Plot of the missing  $E_T$  for opposite sign lepton pairs with one jet.

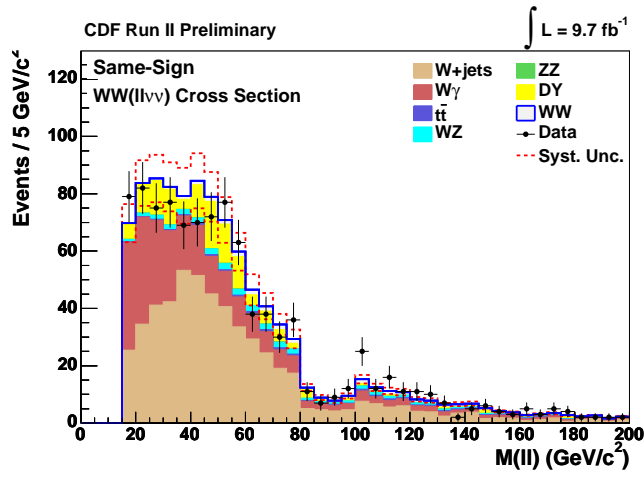


Figure 7: Plot of the invariant mass of same sign lepton pairs.

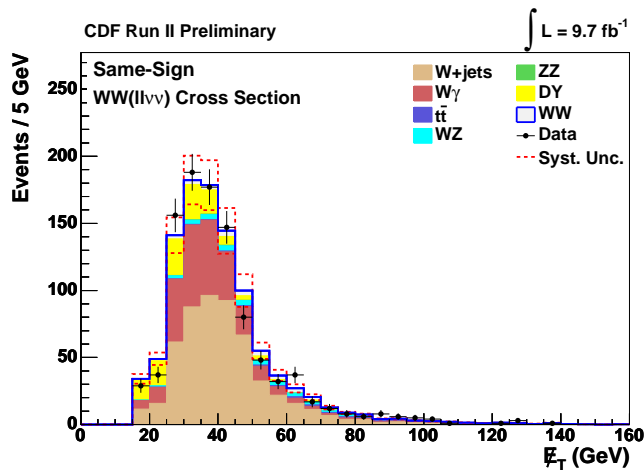


Figure 8: Plot of the missing  $E_T$  for same sign lepton pairs.

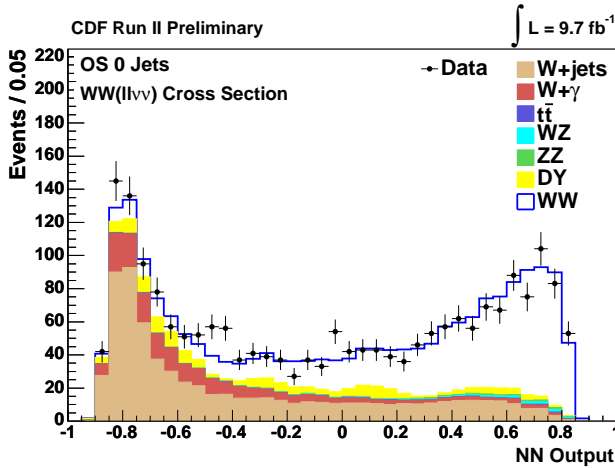


Figure 9: Neural net output for zero jets.

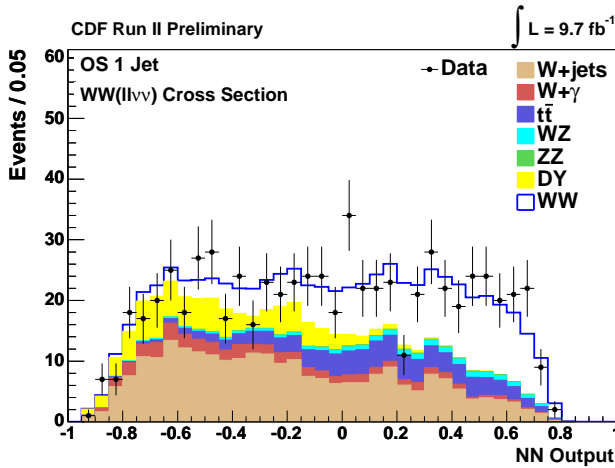


Figure 10: Neural net output for one jet.

scalar  $\Sigma E_T$  is high for top quarks, middle for WW pairs, and lower for other backgrounds.

The neural net output is a single variable in the range  $-1 < x < 1$ . Negative values favor the background, and positive values the signal. Figures 9, 10, and 11 show the NN output for zero jets, one jet, and two or more jets respectively.

Figure 9 shows the classic shape of a neural net output, where the distinction between signal and background is clear. Signal peaks near one, and background near minus one. Figures 10 and 11 not so much, although Fig. 10 does have a broad enhancement for positive output values. Figure 11 is dominated by top quarks, as expected. Last year's discovery is this year's background. The fitted numbers are assembled in Table II.

As seen from the table, the WW signal was about 1/2 of the total in the zero jet bin, 1/3 of the total in the one jet bin, and 1/5 of the total in the two or more jets bin. In order to extract a cross section, these numbers must be corrected for trigger efficiency, detector acceptance, and branching fraction. The integrated luminosity was an important source of systematic uncertainty.[14] Trigger efficiency was obtained from the data, for example by looking at  $Z \rightarrow l^+l^-$ , where one lepton was

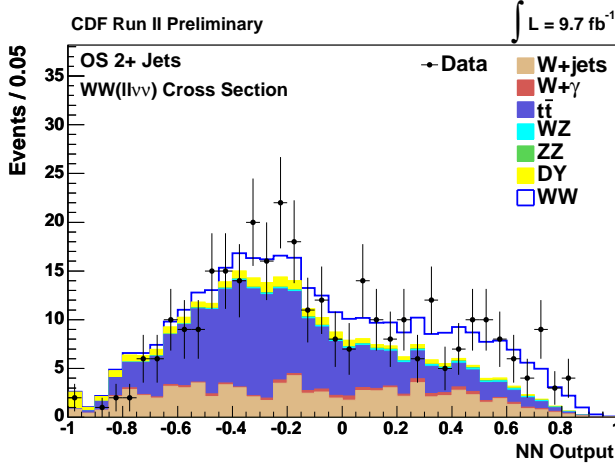


Figure 11: Neural net output for two or more jets.

Table 2: WW (llv) Events best fit CDF Run II Preliminary  $\int Ldt = 9.7\text{fb}^{-1}$

Process	0 Jets	1 Jet	2 or more Jets
WZ	$19.5 \pm 3.0$	$16.6 \pm 2.3$	$4.26 \pm 0.81$
ZZ	$13.2 \pm 1.9$	$4.25 \pm 0.61$	$1.33 \pm 0.26$
$t\bar{t}$	$3.7 \pm 1.0$	$76 \pm 12$	$158 \pm 16$
DY	$150 \pm 34$	$83 \pm 21$	$20.2 \pm 8.6$
$W\gamma$	$214 \pm 27$	$44 \pm 6.4$	$7.5 \pm 1.9$
W+jets	$685 \pm 118$	$250 \pm 46$	$81 \pm 15$
total background	$1086 \pm 124$	$474 \pm 57$	$272 \pm 26$
WW	$963 \pm 108$	$224 \pm 29$	$73 \pm 20$
sig + bckgrnd	$2049 \pm 177$	$698 \pm 73$	$345 \pm 39$
Data	2090	682	331

the trigger, and measuring how often the second lepton also triggered. Lepton identification efficiencies were similarly measured in the data, and used to correct the efficiency in the Monte Carlo simulation. Detector acceptance had to be calculated from the Monte Carlo. PYTHIA generates W decays into  $(e,\nu)$ ,  $(\mu,\nu)$ , and  $(\tau,\nu)$  final states. For W pairs this has a branching fraction  $f = (3 \times 0.108)^2 = 0.105$ . Then the  $e$  or  $\mu$  final state required the appropriate  $\tau$  decay modes, which have a lower acceptance than the direct  $e,\mu$  decays. Adding across the WW fitted signal in Table II gives  $1260 \pm 111$  events. Dividing by  $\int Ldt = 9.7\text{fb}^{-1}$  and 0.105 gives an effective cross section of  $1.24 \pm 0.11$  pb. Comparing this with the quoted result of  $14 \pm 1.2$  pb allows an estimation of the overall acceptance derived from the Monte Carlo:  $\epsilon = 0.088$ .

## 5. Conclusions

Figure 12 shows the final results in graphic form, compared to the latest theoretical expectations. Alpgen is the program developed by Michelangelo Mangano and collaborators [15], while MC@NLO was written by Stefano Frixione and Bryan Webber [16]. The bands show the theoret-

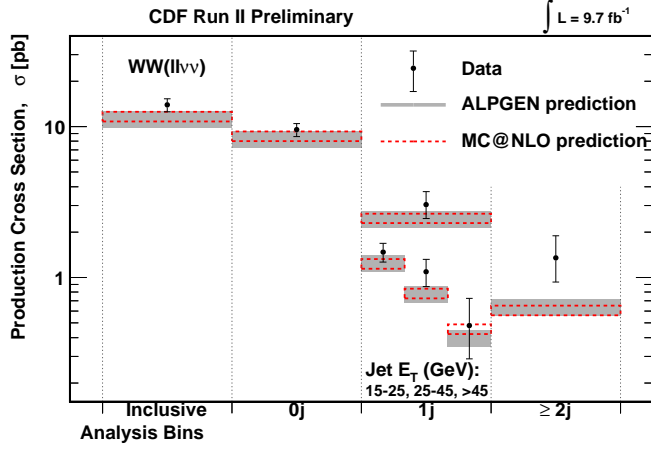


Figure 12: Summary of the results compared to theoretical expectations.

WW(l $\nu\nu$ ) Cross Section	CDF Run II Preliminary			$\int L = 9.7 \text{ fb}^{-1}$		
	$\sigma(\text{pb})$	Uncertainty(pb)		$\sigma(\text{pb})$		
Jet Bin	Measured	Stat.	Syst.	Lumi.	Alpgen	MC@NLO
Inclusive	14.0	$\pm 0.6$	$^{+1.2}_{-1.0}$	$\pm 0.8$	$11.3 \pm 1.4$	$11.7 \pm 0.9$
0 Jets	9.57	$\pm 0.40$	$^{+0.82}_{-0.68}$	$\pm 0.56$	$8.24 \pm 1.04$	$8.62 \pm 0.63$
1 Jet Inclusive	3.04	$\pm 0.46$	$^{+0.48}_{-0.32}$	$\pm 0.18$	$2.43 \pm 0.31$	$2.47 \pm 0.18$
1 jet, $15 < E_T < 25 \text{ GeV}$	1.47	$\pm 0.17$	$^{+0.13}_{-0.09}$	$\pm 0.09$	$1.26 \pm 0.16$	$1.18 \pm 0.09$
1 jet, $25 < E_T < 45 \text{ GeV}$	1.09	$\pm 0.18$	$^{+0.14}_{-0.11}$	$\pm 0.06$	$0.77 \pm 0.10$	$0.79 \pm 0.06$
1 jet, $E_T > 45 \text{ GeV}$	0.48	$\pm 0.15$	$^{+0.19}_{-0.11}$	$\pm 0.03$	$0.40 \pm 0.05$	$0.46 \pm 0.03$
2 or More jets	1.35	$\pm 0.30$	$^{+0.45}_{-0.28}$	$\pm 0.08$	$0.64 \pm 0.08$	$0.61 \pm 0.05$

Table 3: Measured and predicted differential and inclusive cross sections

ical uncertainty, and the bars show the over-all experimental uncertainty. The measurements are systematically high, as were most of the numbers in Table I. Table III summarizes the numbers. The measured total cross section is  $\sigma(p\bar{p} \rightarrow W^+W^- + X) = 14.0 \pm 0.6(\text{stat})^{+1.2}_{-1.0}(\text{syst}) \pm 0.8(\text{lumi})$  pb. Each of the exclusive cross sections shown is within two  $\sigma$  of Standard Model expectations, or better.

## 6. Acknowledgments

We thank the Fermilab staff and the technical staffs of the participating institutions for their vital contributions. This work was supported by the U.S. Department of Energy and National Science Foundation; the Italian Istituto Nazionale di Fisica Nucleare; the Ministry of Education, Culture, Sports, Science and Technology of Japan; the Natural Sciences and Engineering Research Council of Canada; the National Science Council of the Republic of China; the Swiss National Science Foundation; the A.P. Sloan Foundation; the Bundesministerium für Bildung und Forschung, Germany; the Korean World Class University Program, the National Research Foundation of Korea;

the Science and Technology Facilities Council and the Royal Society, UK; the Russian Foundation for Basic Research; the Ministerio de Ciencia e Innovación, and Programa Consolider-Ingenio 2010, Spain; the Slovak R&D Agency; the Academy of Finland; the Australian Research Council (ARC); and the EU community Marie Curie Fellowship contract 302103.

## References

- [1] This report is based on the published work of Will Parker, Proceedings of the 37th International Conference on High Energy Physics, Nuclear Physics B Proceedings Supplement (2014).
- [2] T. Aaltonen *et al.*, (CDF Collaboration) Phys Rev Lett **104**, 201801 (2010).
- [3] V. Abazov *et al.*, (D0 Collaboration) Phys Rev Lett **103**, 191801 (2009).
- [4] Atlas Collaboration, Physics Letters B **712** 289 (2012).
- [5] Atlas Collaboration, ATLAS-CONF 2014-013 (2014).
- [6] CMS Collaboration, Physics Letters B **699** 25 (2011).
- [7] CMS Collaboration, Physics Letters B **721** 190 (2013).
- [8] A. Bhatti *et al.*, Nucl. Instr. Meth. A **566** 375 (2006).
- [9] T. Aaltonen *et al.*, (CDF Collaboration) Phys Rev D **88** 052012, (2013).
- [10] J. Freeman *et al.*, CDF/DOC/CDF/PUBLIC/10803 (2012).
- [11] T. Aaltonen *et al.*, (CDF Collaboration) Phys Rev Lett **94**, 041803 (2005).
- [12] T. Sjostrand *et al.*, Comput. Phys. Commun. **135**, 238 (2001), and **178** 852 (2008).
- [13] M. Feindt and U. Kerzel, Nucl. Instr. Meth. A **559**, 190 (2006).
- [14] D. Acosta *et al.*, Nucl. Instr. Meth. A **494**, 57 (2002).
- [15] M.L. Mangano *et al.*, arXiv:hep-ph/0206093v2 26 May 2003.
- [16] Stefano Frixione and Bryan Webber, JHEP **0206**, 029 (2002), and Frixione, Nason, and Webber, JHEP **0308**, 007 (2003).